Metasurface Head Volume Coil for 10.5 T MRI

Léo Rémillard[1], Christopher J. M. Barker[2], Ashwin K. Iyer[2], Nicola De Zanche[1]
[1]Dept. of Medical Physics and Dept. of Oncology, University of Alberta, Edmonton AB, Canada, [2]Dept. of Electrical and Computer Engineering, University of Alberta, Edmonton AB, Canada

UNIVERSITY OF ALBERTA

INTRODUCTION

Purpose

Interest in ultrahigh field (UHF) MRI is constantly growing due to its increased SNR and higher resolution. This leads to improved image quality, which has plenty of potential to affect clinical work by allowing more precise contouring of brain tumors, and better detection of brain lesions in stroke patients as well as letting researchers resolve the fine cortical structures of the brain [1, 2, 3]. However, the advantages of UHF MRI are balanced by drawbacks such as the increased radiofrequency (RF) field inhomogeneity due to standing wave effects, which result in dark regions over anatomy in images and increased energy deposition in tissue. The most common method of counteracting these issues is parallel transmit (pTx), where the phase and magnitude of the RF pulse train sent to each coil is optimized. While this method is successful, it requires the computational resources to perform the optimization, and can increase scan times if pre-scans are necessary. Designing a coil that can avoid generating these inhomogeneities would thus simplify the UHF imaging workflow.

Hypothesis

Metamaterials and metasurfaces (MTSs) have successfully been employed at lower field strengths to counteract RF field inhomogeneities both as passive shimming devices and as coils [4, 5, 6]. The hypothesis is that the success at lower field strengths can be translated to UHF MRI, and that a MTS head coil can achieve the same sensitivity or greater when compared to preexisting coil arrays at 10.5 T.

THEORY

A MTS is a 2D structure composed of many subwavelength unit cells which act together to exhibit largescale electromagnetic properties. Acting as an impedance/admittance boundary, the MTS can modify the dispersion inside a waveguide. A MTS design for controlling dispersion in a cylindrical waveguide in the gigahertz regime is adapted for use in 10.5 T MRI (447 MHz), with the coil RF shield acting as a waveguide [7]. Through proper design, the MTS can allow an MR conducive mode with a uniform transverse B field to resonate in the RF shield below the natural cutoff (627.5 MHZ). Here each unit cell is a conductive cross with capacitors between each cell. The capacitor values determine the impedance of the MTS and thus the resonant frequency.

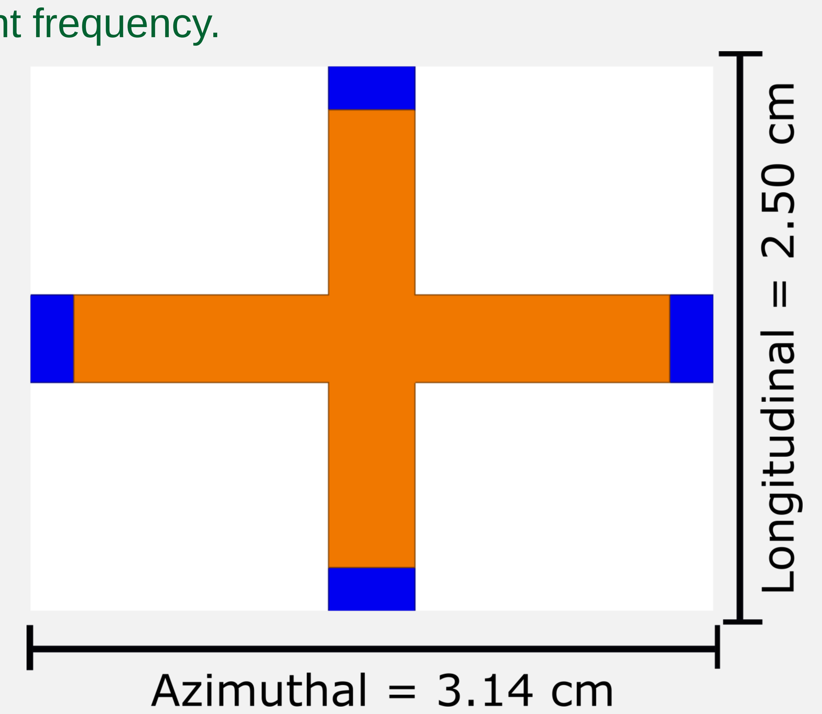

Figure 1: A unit cell of the MTS. The blue rectangles are lumped capacitors, and the orange traces are conductors.

METHODS

Dimensions

Coil Dimensions: 30 cm length, 28 cm diameter
RF Shield Diameter: 31 cm

Simulations

Software: Ansys HFSS
Eigenmode simulations are used to rapidly determine initial capacitor values from only a single MTS ring. Full wave simulations are then used to fine tune the coil as the finite dimensions affect the tuning. A 17 cm in diameter "lightbulb" phantom with ε_r = 47.26, σ = 0.65 S/m simulates a human head. Circuit co-simulations are performed with CoSimPy if needed [8].

Imaging

Use Siemens MAGNETOM 10.5 T scanner at the University of Minnesota at a later date.

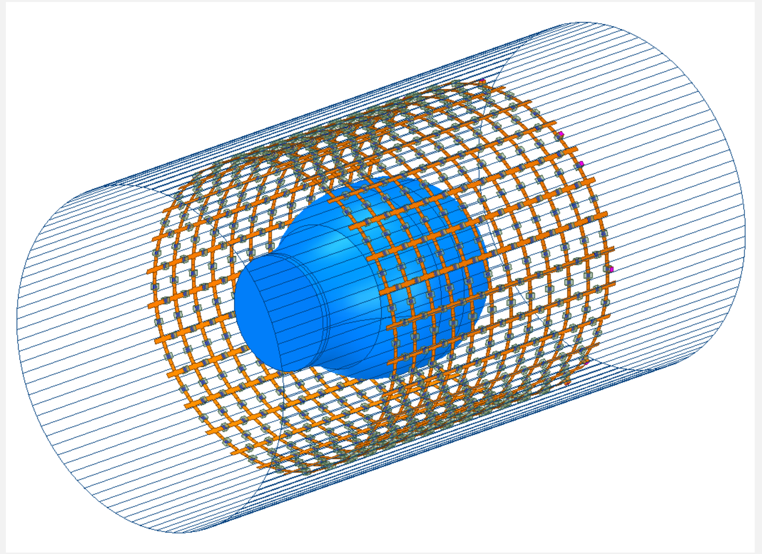

Figure 2:The full wave simulation setup. The orange structure is the MTS, the blue volume is the phantom, and the outermost cylinder represents the coil's RF shield.

RESULTS

Ports are decoupled and matched by renormalizing the port impedance in HFSS. The fields are then exported and analyzed in MATLAB. A sphere 3 cm in diameter is centered in the phantom and used to calculate the mean transmit sensitivity and standard deviation in the region

Simulations: Unloaded

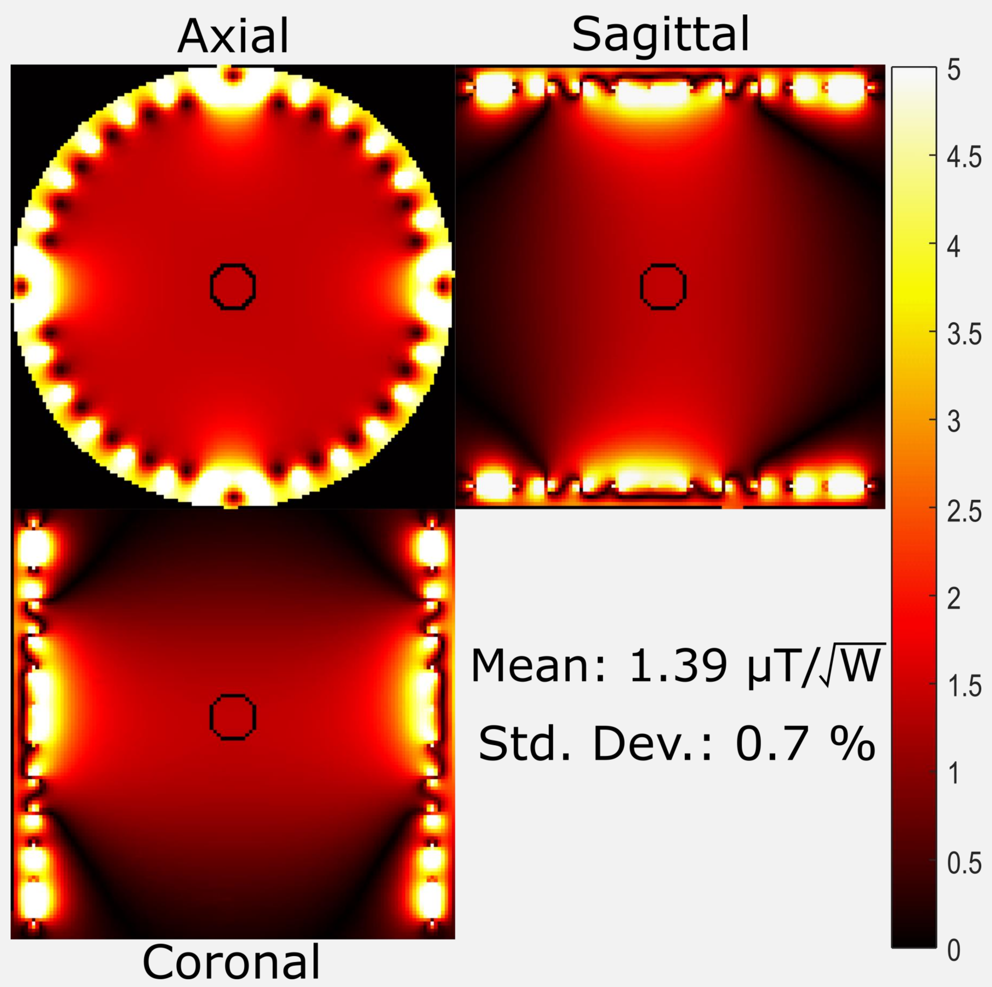

Figure 3: Transmit sensitivity plots of the unloaded MTS coil. A very homogeneous region is present in the center of the coil. This region is very slightly shifted towards the rear of the coil due to the asymmetry of the coil acquired from slight tuning adjustments. The mean is calculated inside the 3 cm sphere outlined in black.

Simulations: Loaded

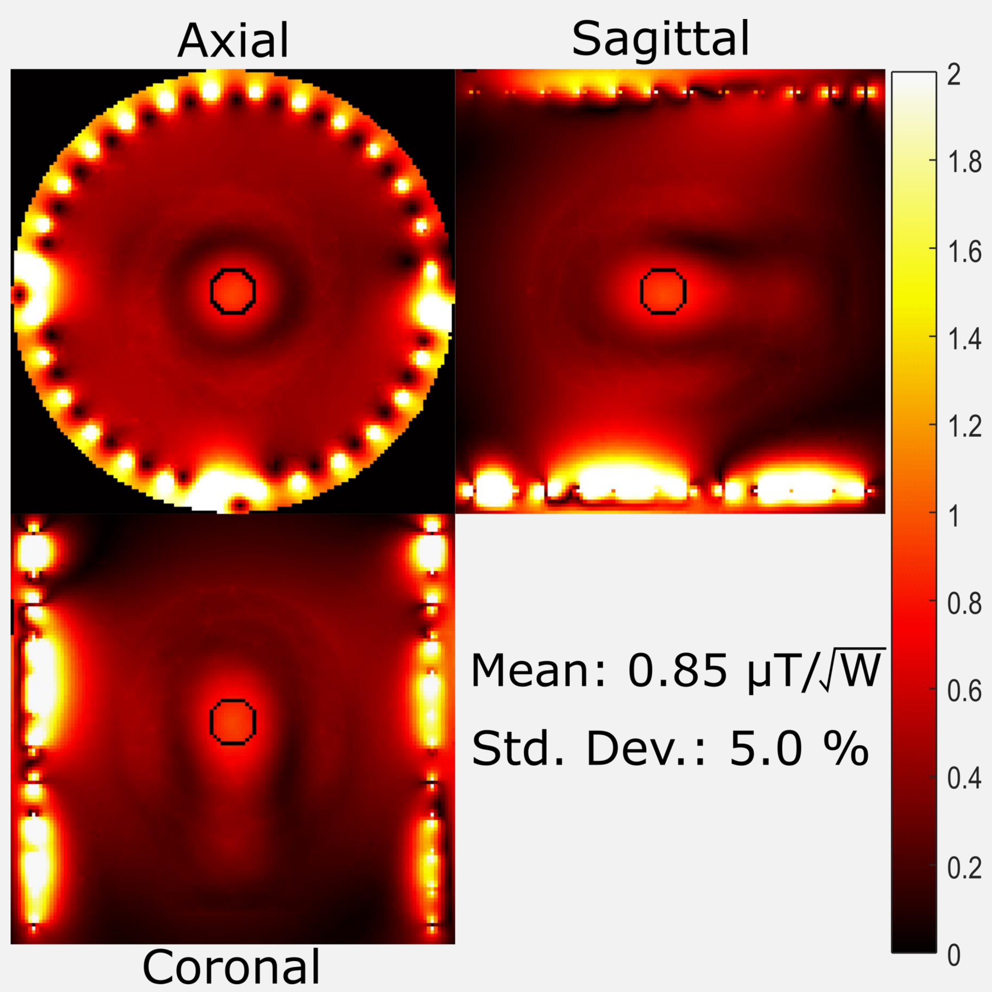

Figure 4: Transmit sensitivity plots of the loaded MTS coil. A region with strong sensitivity and good homogeneity is present in the center of the phantom surrounded by a low sensitivity region due to wave interference. The mean is calculated in a 3 cm diameter sphere in the center of the phantom.

RESULTS CONT.

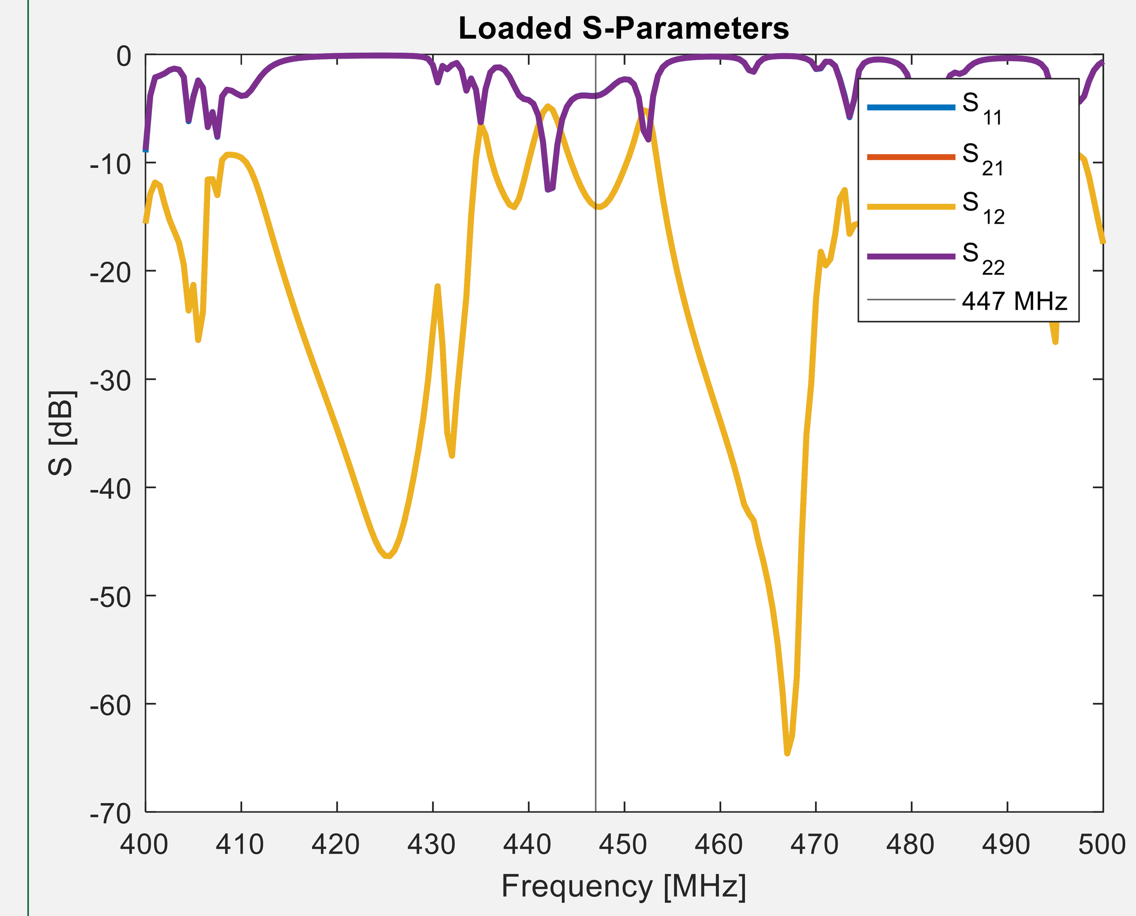

Figure 5: S parameters of coil with renormalized port impedances. High S_{11} and S_{22} show that the tuning has not been optimized.

DISCUSSION/CONCLUSION

Discussion

Final capacitor values used were C_{phi} = 3.3 pF and C_z = 5.8 pF. The transmit sensitivity values are similar to those of standard transmit coil arrays of 0.68 to 0.73 μT/√W with qualitatively similar inhomogeneities [9, 10].

Conclusion

From the simulation results, the MTS head coil performs similarly to conventional UHF head coil arrays.

REFERENCES

[1] S. Regnery *et al.*, "High-resolution FLAIR MRI at 7 Tesla for treatment planning in glioblastoma patients," *Radiotherapy and Oncology*, vol. 130, pp. 180–184, Jan. 2019, doi: 10.1016/j.radonc.2018.08.002.
[2] V. Novak, A. M. Abduljalil, P. Novak, and P. M. Robitaille, "High-resolution ultrahigh-field MRI of stroke," *Magnetic Resonance Imaging*, vol. 23, no. 4, pp. 539–548, May 2005, doi: 10.1016/j.mri.2005.02.010.
[3] V. G. Kemper, F. De Martino, T. C. Emmerling, E. Yacoub, and R. Goebel, "High resolution data analysis strategies for mesoscale human functional MRI at 7 and 9.4T," *NeuroImage*, vol. 164, pp. 48–58, Jan. 2018, doi: 10.1016/j.neuroimage.2017.03.058.
[4] A. M. Maunder, C. Barker, N. De Zanche, and A. K. Iyer, "Metamaterial Liner for MRI Excitation—Part 1: Theory, Modeling and Design," *IEEE Access*, vol. 10, pp. 41664–41677, 2022, doi: 10.1109/ACCESS.2022.3167432.
[5] A. M. Maunder, A. K. Iyer, and N. De Zanche, "Metamaterial Liner for MRI Excitation—Part 2: Design and Performance at 4.7T," *IEEE Access*, vol. 10, pp. 41678–41692, 2022, doi: 10.1109/ACCESS.2022.3167764.
[6] L. Smart, A. M. Maunder, A. K. Iyer, and N. De Zanche, "The Metaslab: A combined Metamaterial and Metasurface for Improved Transmit Performance and Use as a Receive Array," in *Proceedings of the International Society for Magnetic Resonance in Medicine*, Toronto, Canada, 2023, p. 3899.
[7] C. J. M. Barker, N. De Zanche, and A. K. Iyer, "Dispersion and Polarization Control in Below-Cutoff Circular Waveguides Using Anisotropic Metasurface Liners," *IEEE Transactions on Microwave Theory and Techniques*, vol. 71, no. 8, pp. 3392–3403, Aug. 2023, doi: 10.1109/TMTT.2023.3263396.
[8] U. Zanovello, F. Seifert, O. Bottauscio, L. Winter, L. Zilberti, and B. Ittermann, "CoSimPy: An open-source python library for MRI radiofrequency Coil EM/Circuit Cosimulation," *Computer Methods and Programs in Biomedicine*, vol. 216, p. 106684, Apr. 2022, doi: 10.1016/j.cmpb.2022.106684.
[9] M. K. Woo *et al.*, "A 16-Channel Dipole Antenna Array for Human Head Magnetic Resonance Imaging at 10.5 Tesla," *Sensors*, vol. 21, no. 21, Art. no. 21, Jan. 2021, doi: 10.3390/s21217250.
10] M. K. Woo *et al.*, "Evaluation of a 16-Channel Transceiver Loop + Dipole Antenna Array for Human Head Imaging at 10.5 Tesla," *IEEE Access*, vol. 8, pp. 203555–203563, 2020, doi: 1 0.1109/ACCESS.2020.3036598.

Contact Information:

Email: lremilla@ualberta.ca

Acknowledgments:

I would like to thank Dr. Adam Maunder for lending his expertise to this porject. I would also like to thank our collaborators from the University of Minnesota Dr. Gregor Adriany and Russell Lagore.

References:

[1] S. Regnery *et al.*, “High-resolution FLAIR MRI at 7 Tesla for treatment planning in glioblastoma patients,” *Radiotherapy and Oncology*, vol. 130, pp. 180–184, Jan. 2019, doi: 10.1016/j.radonc.2018.08.002.

[2] V. Novak, A. M. Abduljalil, P. Novak, and P. M. Robitaille, “High-resolution ultrahigh-field MRI of stroke,” *Magnetic Resonance Imaging*, vol. 23, no. 4, pp. 539–548, May 2005, doi: 10.1016/j.mri.2005.02.010.

[3] V. G. Kemper, F. De Martino, T. C. Emmerling, E. Yacoub, and R. Goebel, “High resolution data analysis strategies for mesoscale human functional MRI at 7 and 9.4T,” *NeuroImage*, vol. 164, pp. 48–58, Jan. 2018, doi: 10.1016/j.neuroimage.2017.03.058.

[4] A. M. Maunder, C. Barker, N. De Zanche, and A. K. Iyer, “Metamaterial Liner for MRI Excitation—Part 1: Theory, Modeling and Design,” *IEEE Access*, vol. 10, pp. 41664–41677, 2022, doi: 10.1109/ACCESS.2022.3167432.

[5] A. M. Maunder, A. K. Iyer, and N. De Zanche, “Metamaterial Liner for MRI Excitation—Part 2: Design and Performance at 4.7T,” *IEEE Access*, vol. 10, pp. 41678–41692, 2022, doi: 10.1109/ACCESS.2022.3167764.

[6] L. Smart, A. M. Maunder, A. K. Iyer, and N. De Zanche, “The Metaslab: A combined Metamaterial and Metasurface for Improved Transmit Performance and Use as a Receive Array,” in *Proceedings of the International Society for Magnetic Resonance in Medicine*, Toronto, Canada, 2023, p. 3899.

[7] C. J. M. Barker, N. De Zanche, and A. K. Iyer, “Dispersion and Polarization Control in Below-Cutoff Circular Waveguides Using Anisotropic Metasurface Liners,” *IEEE Transactions on Microwave Theory and Techniques*, vol. 71, no. 8, pp. 3392–3403, Aug. 2023, doi: 10.1109/TMTT.2023.3263396.

[8] U. Zanovello, F. Seifert, O. Bottauscio, L. Winter, L. Zilberti, and B. Ittermann, “CoSimPy: An open-source python library for MRI radiofrequency Coil EM/Circuit Cosimulation,” *Computer Methods and Programs in Biomedicine*, vol. 216, p. 106684, Apr. 2022, doi: 10.1016/j.cmpb.2022.106684.

[9] M. K. Woo *et al.*, “A 16-Channel Dipole Antenna Array for Human Head Magnetic Resonance Imaging at 10.5 Tesla,” *Sensors*, vol. 21, no. 21, Art. no. 21, Jan. 2021, doi: 10.3390/s21217250.

[10] M. K. Woo *et al.*, “Evaluation of a 16-Channel Transceiver Loop + Dipole Antenna Array for Human Head Imaging at 10.5 Tesla,” *IEEE Access*, vol. 8, pp. 203555–203563, 2020, doi: 10.1109/ACCESS.2020.3036598.